

Interaction of the laser with the material - modelling of the microlenses creation

P. Janicek^{1,2,*}, P. Kutalek³, J. Schwarz⁴, J. Smolik³, P. Knotek⁴

1. Institute of Applied Physics and Mathematics

2. Center of Materials and Nanotechnologies

3. Joint Laboratory of Solid State Chemistry

4. Department of General and Inorganic Chemistry

all at Faculty of Chemical Technology, University of Pardubice, Studentska 95, 532 10, Pardubice, Czech Republic

*The corresponding author e-mail: petr.janicek@upce.cz

Abstract

Microlenses with potential applications in optics on the surface of the various heavy-metal oxide glasses were created and studied experimentally. Laser direct writing using continuous-wave laser emitting at 447 nm was successfully performed for PbO-Bi₂O₃-Ga₂O₃ glasses. This study aims to compare the height and spatial profile of microlenses numerically calculated using COMSOL with the experimental results measured by holographical and atomic force microscopy. The role of different parameters (laser power density, exposition time, etc.) on the microlenses is discussed.

Development of the thermal model obtained by utilization of Localized Heat Source application to Radiative Beam in Absorbing Media Interface with thermal expansion using COMSOL 6.1. is shown and compared with experimental results. Utilizing Heat transfer module in COMSOL 6.1. allows us to calculate the local temperature during the laser illumination in the different places on the sample in dependence on illumination time. In combination with the thermal expansion using Structural Mechanics module, local displacement (corresponding to local height of the microlenses) can be calculated.

Keywords: microlenses, local over-heating, laser-induced, Heat transfer, thermal expansion.

Introduction

Heavy metal oxide glasses containing a significant amount of oxides of heavy metals (in our case Pb (2+) or Bi (3+)) possess the high value of the refractive index, good transmission in the infrared region (up to 7-8 μm), high value of non-linear refractive index, low value of glass transition temperature T_g , high coefficient of thermal expansion CTE and also good chemical stability [1-2]. These parameters allow their utilization in optics. Recently we reported the development/preparation of microlenses with potential applications in optics on the surface of the various heavy-metal oxide glasses with the composition PbO-Bi₂O₃-Ga₂O₃ [1-2]. Microlenses were formed by laser direct writing using continuous-wave laser emitting at 447 nm [2]. The aim of this study is to compare the height and spatial profile of microlenses numerically calculated using COMSOL with the measured results performed using holographical and atomic force microscopy. In this study, we would like to describe used COMSOL model in more detail together with the role of different parameters (laser power density, exposition time etc.) on the microlenses formation.

Theory / Experimental Set Up

There are more approaches how to model interaction of laser with the material described in COMSOL blog [3]. The simplest way is

considering laser as the heat dissipated either as point source or as heat source with defined radius. For this purpose, Heat Conduction with a Localized Heat Source on a Disk (Application ID: 17307) was used (see figure 1) for which Heat Transfer Module is necessary. Although 2D model is used its 3rd dimension representing thickness of the sample can also be varied. If certain diameter of the heat source is used than in 3D this model represents cylindrical heat source.

In our study, the absorption coefficient depends on the composition. In order to include absorption coefficient, Modeling Laser Beam Absorption in Silica Glass with Beer-Lambert Law (Application ID: 56101) is more appropriate.

Using this approach time dependent spatial distribution of temperature can be modelled. Our assumption is that microlens on the surface is created due to thermal expansion connected with local overheating. Last step is therefore to include thermal expansion. Because we do not have access to Structural Mechanics Module, Thermal Microactuator Simplified (Application ID: 16357) was used, Thermal expansion is included, in this case, by editing the equations in Equation View rather than by using a multiphysics coupling and does not require any add-on licenses (Heat Transfer module is sufficient).

Governing Equations / Numerical Model / Simulation / Methods / Use of Simulation Apps

In the first step, modified Heat Conduction with a Localized Heat Source on a Disk (Application ID: 17307) model was used to estimate increase of temperature. Schematic view for used geometry is in figure 1.

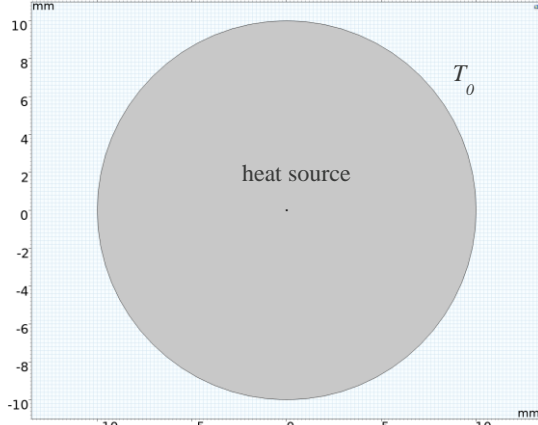


Figure 1. Used model for Localized heat source. Small circle in the centre represents laser as the heat source.

In this case stationary solution (spatial distribution of temperature T) of Heat transfer equation

$$\nabla \cdot (-k\nabla T) = Q\delta$$

is solved where k is thermal conductivity and δ represents Dirac distribution. $Q = P/d_z$ represents volumetric heat source with power of dissipated heat P (power of laser in the first approximation) and thickness of the sample d_z (in z direction perpendicular to xy plane in figure 1). Constant temperature T_0 was used as boundary condition on the outside of the disc (see figure 1).

Temperature dependence of material properties (Heat capacity C_p and thermal conductivity k) is included via Definition -> Interpolation where several experimental values were used (see figures 11-12 in Appendix).

To include also absorption coefficient Modeling Laser Beam Absorption in Silica Glass with Beer-Lambert Law (Application ID: 56101) was used. For this purpose, 2D axisymmetric component with $r = 0$ being axis of rotation is useful as shown in figure 2 allowing to display results in 3D figure.

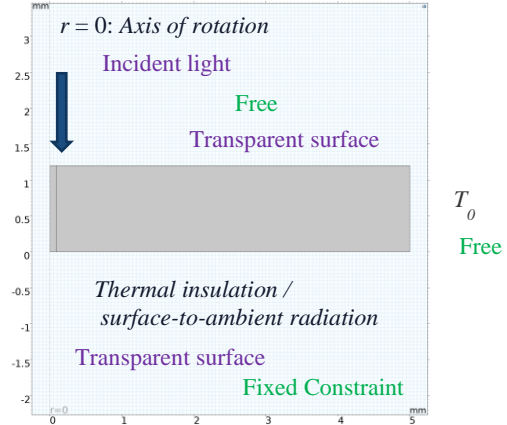


Figure 2. Used model for Beer-Lambert Law.

Here time (t) dependent Heat transfer equation

$$\rho C_p \frac{\partial T}{\partial t} - \nabla \cdot (k\nabla T) = Q_r$$

is solved using density ρ , heat capacity C_p and thermal conductivity k as material parameters to get radial and depth distribution of temperature (T) within a defined time. Heat source Q_r depends on the intensity of the light I via (temperature dependent) absorption coefficient κ

$$Q_r = \kappa(T)I$$

and dependence of intensity on depth is given using Beer-Lambert Law (\vec{e} is the unit vector)

$$\frac{\vec{e}}{\|\vec{e}\|} \cdot \nabla I = -\kappa(T)I$$

For this purpose, Heat transfer module using Radiative Beam in Absorbing Media Interface can be used. Multiphysics coupling allows calculating intensity of the light in different material's depths which causes heating of the material also for the case where the absorption coefficient depends on the temperature. Moreover, laser beam profile can be defined by a user, or a standard Gaussian or top-hat beam profile can be applied.

Top-hat laser profile was adopted with spatial distribution of the intensity of the light given by

$$f(\vec{O}, \vec{e}) = \frac{1}{\pi R^2}, \text{ if } d \leq R$$

$$f(\vec{O}, \vec{e}) = 0, \text{ if } d > R$$

where $d = \frac{\|\vec{e} \times (\vec{x} - \vec{O})\|}{\|\vec{e}\|}$ and beam orientation \vec{e} ,

together with beam origin point \vec{O} and beam radius $R = d/2$ are the parameters defined by the user.

For Gaussian profile

$$f(\vec{O}, \vec{e}) = \frac{1}{2\pi\sigma^2} \exp\left(-\frac{d^2}{2\sigma^2}\right)$$

with standard deviation σ .

Constant temperature T_0 was utilized as a boundary condition on the outside of the disc in accordance with previously used Heat Conduction with a Localized Heat Source on a Disk. Thermal insulation was applied on lower boundary and surface-to-ambient radiation / thermal insulation on upper boundary (labelled by black color in figure 2). In addition to incident light with top-hat profile transparent surface boundary condition was used for the rest of upper boundary and also for bottom

boundary for Radiative Beam in Absorbing Media (labelled by magenta color in figure 2).

To include thermal expansion without having access to Structural module Thermal Microactuator Simplified (Application ID: 16357) was utilized. Here local strain ε defined using local displacement vector \vec{u} depends on (temperature dependent) coefficient of thermal expansion CTE as

$$\varepsilon = CTE(T) \cdot dT = \vec{\nabla} \cdot \vec{u}$$

and local increase in height z can be calculated as

$$d\Delta z = CTE(T) \cdot dT \cdot \Delta z_0$$

Within this approach new physics Solid Mechanics which is part of COMSOL core is added and in the Equation View for Linear elastic material following equation

$$solid.eZZ = wZ - CTE(T) * (T - T_0)$$

is used allowing material to expand in z - direction. More details about this approach can be found in COMSOL blog [4].

For Solid state mechanics Fixed Constraint at lower boundary together with Free upper and right boundary was used (labelled by green color in figure 2).

Adding all these together, geometrically relatively simple model depicted in figure 2 was used. Division of the rectangle in 2D axisymmetric model to two parts – one representing the illuminated area and second the rest of the sample – was also used to have different mesh in both parts. Mesh used in the illuminated part is much finer as most of the physics is expected to take part in it.

Experimental Results / Simulation Results / Discussion

As described above, first approximation of temperature overheating was done using Heat Conduction with a Localized Heat Source on a Disk (Application ID: 17307). Used parameters are in Table 1 representing $(PbO)_{0.75}(Ga_2O_3)_{0.25}$ (PBG0) bulk glass [2] and its schematic presentation in fig. 1.

Table 1: Parameters for Localized Heat Source on a Disk (Application ID: 17307)

Parameter	Quantity
Diameter of the sample	10 mm
Diameter of laser (heat source)	0.2 mm
Surrounding temperature T_0	300 K
Out-of-plane thickness d_z	1 mm
Heat capacity C_p	351 J/(kgK)
Thermal conductivity k	0.58 W/(mK)
Density ρ	7520 kg/m ³

Geometrical and material parameters obtained from experiment were used [2]. Firstly, constant values were used, temperature dependence of heat capacity

and thermal conductivity in the following step (see figures 11-12 in Appendix).

From this calculation temperature overheating $T-T_0$ about 300 K can be expected for laser power 0.2 W and about 600 K for laser power 0.4 W. One of the possible graphical representations for the spatial distribution of temperature using laser power 0.2 W is depicted in figure 3 for constant parameters summarized in Table 1 (stationary solution).

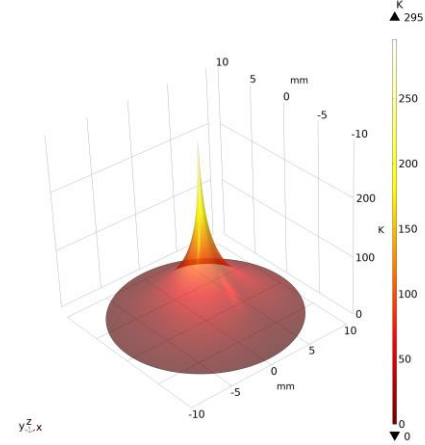


Figure 3. Spatial distribution of temperature overheating $T-T_0$ using laser power 0.2 W for sample with parameters from table 1.

Considering that glass transition temperature T_g of used material is about 400 °C, softening temperature T_s slightly higher ($T_s \approx T_g + 25$) and laser power densities up to 1800 W/cm² are experimentally available these results show usability of this model for studied materials. Notice that experimentally measured diameter of the illuminated spot is $(180 \pm 10) \mu\text{m}$.

To include (temperature dependent) absorption coefficient Modeling Laser Beam Absorption in Silica Glass with Beer-Lambert Law (Application ID: 56101) was used (see figure 2). From the experiment penetration depth d_p is known and absorption coefficient $\kappa = 1/d_p$. Example of the spatial distribution of the temperature for the stationary solution is depicted at in figure 4 for penetration depth $d_p = 318 \mu\text{m}$ corresponding to PBG0 sample [2] together with contours of constant temperature.

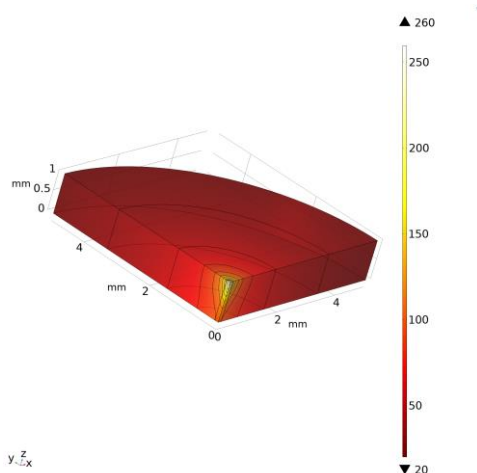


Figure 4. Spatial distribution of temperature using laser power 0.2 W for sample with parameters from table 1 and penetration depth 318 μm .

The main difference between figure 3 (Localized Heat Source) and Figure 4 (Application of Beer-Lambert Law) is that temperature rises only in part of the thickness of the sample and this part contributes to thermal expansion, i.e. creation of the microlens. Moreover, when the maximal temperature is higher than softening temperature T_s the deformation of the microlens and additionally creation of the micro-crater can be expected for temperatures above melting point (typically around 600 $^{\circ}\text{C}$ for $\text{PbO-Bi}_2\text{O}_3\text{-Ga}_2\text{O}_3$ glasses, respectively 759 $^{\circ}\text{C}$ for PBGO [2]).

We assume that local overheating contributes to the creation of the microlens via thermal expansion of the material. Adopting idea from Thermal Microactuator Simplified (Application ID: 16357) the spatial distribution of the temperature within the sample together with total deformation = thermal expansion can be visualised (see figure 5 for PBGO as an example). The scale for deformation is enlarged in order to be visible in the same figure together with realistic dimensions for the sample. Temperature profiles in different depths of illuminated material can be also obtained showing that the overheating quickly diminishes with the depth in the material. For these results temperature dependence of material parameters was used (see figs. 11-14 in Appendix) [2]. Penetration depth and consequently absorption coefficient depend on temperature only slightly (see figure 13 in Appendix).

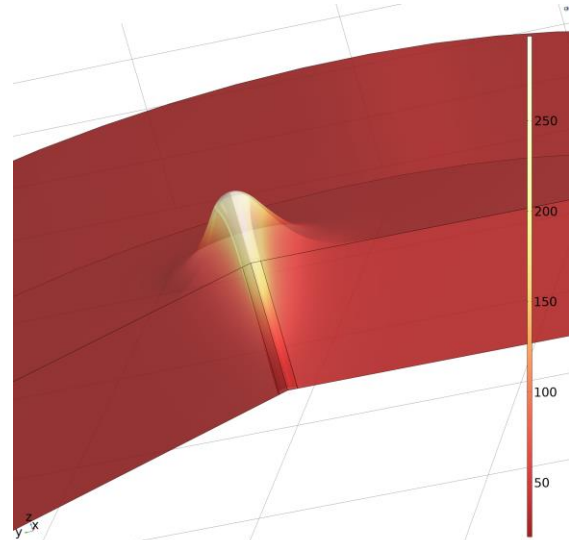


Figure 5. Example of spatial distribution of temperature using laser power 0.1 W for 0.5 s together with total calculated displacement created by thermal expansion for PBGO sample. Notice different scale for deformation.

Taking into account that typical experimental illumination time is about 0.5 s utilization of above-described model allows to study dependence of different parameters. Firstly, fast increase of the temperature on the surface in the centre of the illuminated spot (within 0.1 s) and following heat transfer associated with temperature increase can be visualised for PBGO sample (figure 6).

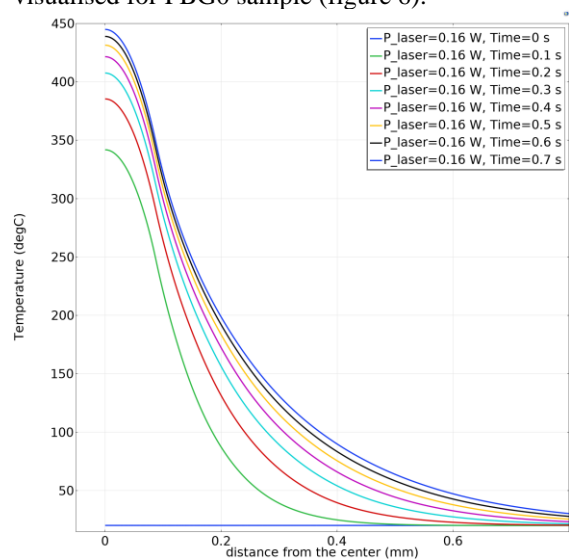


Figure 6. Dependence of the temperature on the surface of the PBGO sample on the distance from the centre for different illumination times and fixed laser power.

Total displacement corresponding to the height of the microlens reflects calculated temperature distribution depicted in figure 6. One can note creation of the crater in the center of the microlens (illuminated spot) for times higher than 0.5 s (black and blue line in figure 7). This is when local temperature exceeds softening temperature (close to glass transition temperature). In the first approximation for temperatures higher than T_s coefficient of thermal expansion CTE was set to

zero in the model (see figure 14 in Appendix). One can also notice faster increase of the height of the microlens when the temperature is slightly below T_g corresponding to the experimentally found increase of CTE (e.g. 4-times higher in the case of PBG0 - see figure 14 in Appendix).

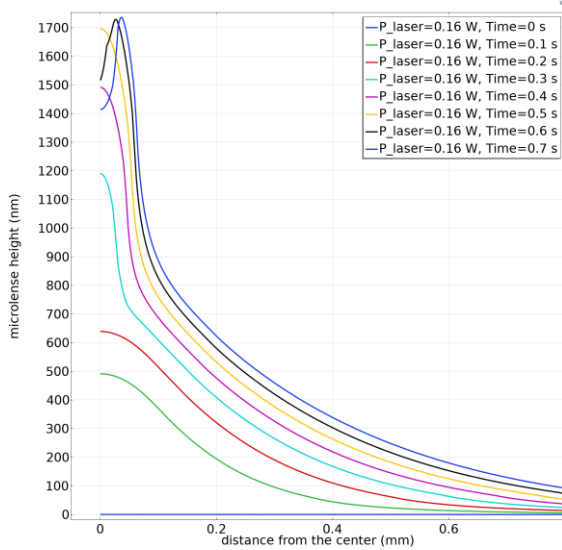


Figure 7. Dependence of total displacement (=height of the microlens) on the distance from the centre for different illumination times and fixed laser power density for PBG0 sample.

Dependence of total displacement on the laser power (after 0.5 s illumination) looks similar (fig. 8). For higher laser powers the maximal temperature exceeds T_s and the microlens is no longer compact.

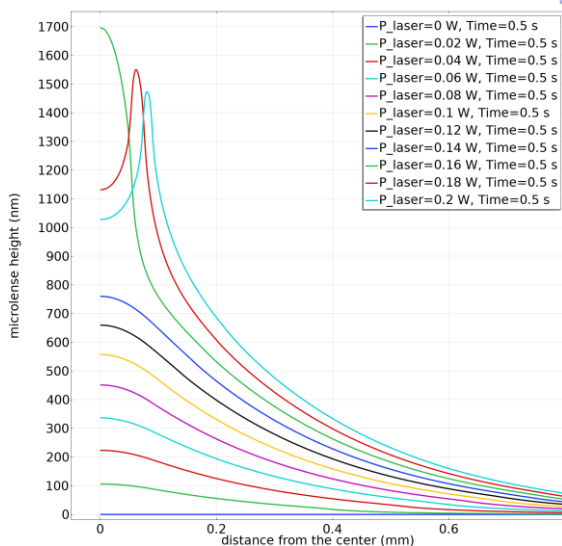


Figure 8. Dependence of total displacement (=height of the microlens) on the distance from the centre for different laser power (illumination time is constant) for PBG0 sample.

Described results correspond well to profile of the microlens obtained experimentally (see figure 9) [2].

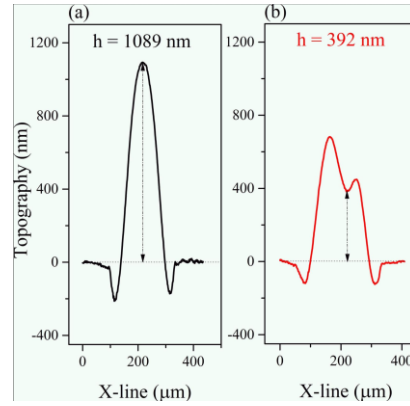


Figure 9. Experimentally observed profiles for (a) microlens, (b) "dimple" microlens after the collapse of its center. Both for PBG2 sample [2].

Dependence of total displacement in defined point (center of the sample on its surface) on laser power (using constant illumination time) is depicted in fig. 10. Increasing laser power increases displacement until the point when the local / maximal temperature exceeds T_s . Decrease of total displacement (=microlens height) for further increase in laser power can be noticed. In this sense, the maximal possible height of the created microlens can be modelled.

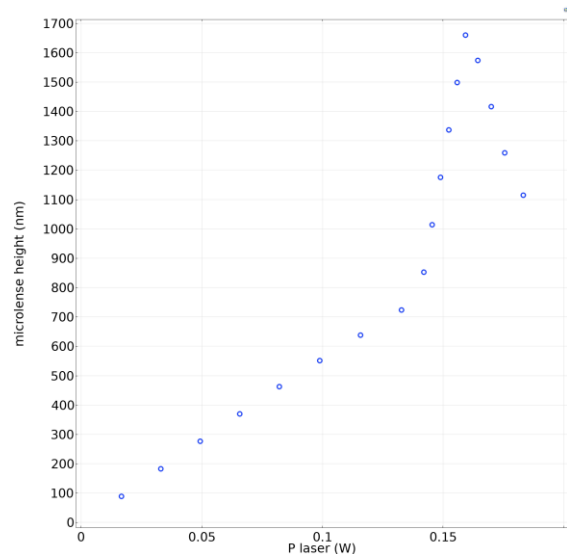


Figure 10. Dependence of total displacement (=height of the microlens) for point in the centre of the illuminated spot on the surface of the sample on the laser power (illumination time is constant) for PBG0 sample.

Overall maximal height of the created microlens is higher from the model than from the experiment. We tend to believe that this discrepancy can be explained by structural relaxation after the illumination causing decrease of photo-induced deformation as was proved in chalcogenide glasses, see figure 9 in [5]. It is worth to mention that the presented model does not fully correspond to experimentally found dependence of microlens height h on laser power density F

$$h = d_{p,eff} \cdot \ln \frac{F}{F_{th}}$$

where $d_{p,eff}$ means the effective optical penetration depth and F_{th} is the threshold value of the laser power density for the microlens formation as the cooling connected with the relaxation is not solved up to now.

Conclusions

Combination of Heat Transfer Module + Radiative Beam in Absorbing Media multiphysics + Solid Mechanics (which is part of COMSOL Multiphysics core) is able to describe spatial distribution of temperature in the material after its illumination by laser and also creation of microlens due to thermal expansion. It is possible to incorporate temperature dependence of material properties into the model showing its influence on the results. Estimated maximal height of the microlens is higher than experimental for PbO-Bi₂O₃-Ga₂O₃ glass due to the relaxation of the glass after switching off the laser. In our next study we would like to focus also on the flow of the viscous glass present when the temperature is above glass transition temperature / softening temperature.

References

- [1] J. Smolik, P. Knotek, J. Schwarz, E. Cernoskova, P. Kutalek, V. Kralova, L. Tichy: Laser direct writing into PbO-Ga₂O₃ glassy system: Parameters influencing microlenses formation, *Applied Surface Science*, pp. 148368, volume 540, 2021.
- [2] J. Smolik, P. Knotek, J. Schwarz, E. Cernoskova, P. Janicek, K. Melanova, L. Zarybnicka, M. Pouzar, P. Kutalek, J. Stanek, J. Edlman, L. Tichý: 3D micro-structuring by CW direct laser writing on PbO-Bi₂O₃-Ga₂O₃ glass, *Applied Surface Science*, pp. 152993, volume 589, 2022.
- [3] <https://www.comsol.com/blogs/modeling-laser-material-interactions-in-comsol-multiphysics/>
- [4] <https://www.comsol.com/blogs/performing-a-multiphysics-analysis-of-a-thermal-microactuator/>
- [5] P. Kutalek, E. Samsonova, J. Smolik, P. Knotek, J. Schwarz, E. Cernoskova, P. Janicek, L. Tichy: Microlenses formation on surface of stoichiometric Ge-As-S bulk glasses by CW laser direct writing, *Applied Surface Science*, pp. 157380, volume 628, 2023.

Acknowledgements

The financial support from the Czech Science Foundation (GA CR), project No. 19-11814S is highly appreciated. This work was supported by the Ministry of Education, Youth, and Sports of the Czech Republic, grant number LM2018103. Support from the Faculty of Chemical Technology, University of Pardubice (FChT UPa) is acknowledged by the authors.

Appendix

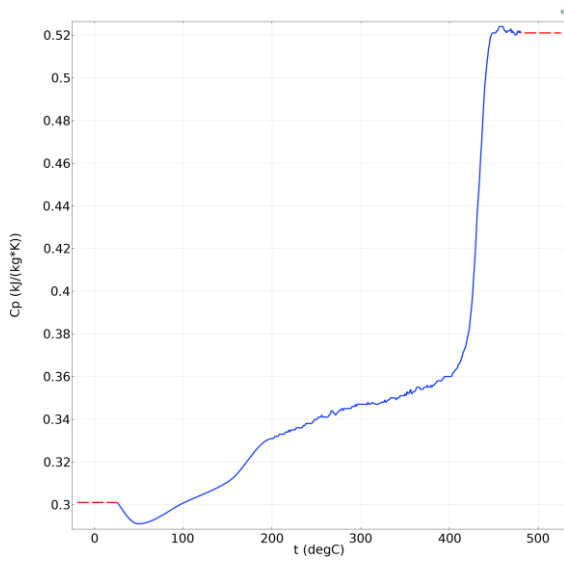


Figure 11. Temperature dependence for heat capacity C_p for PBGO sample.

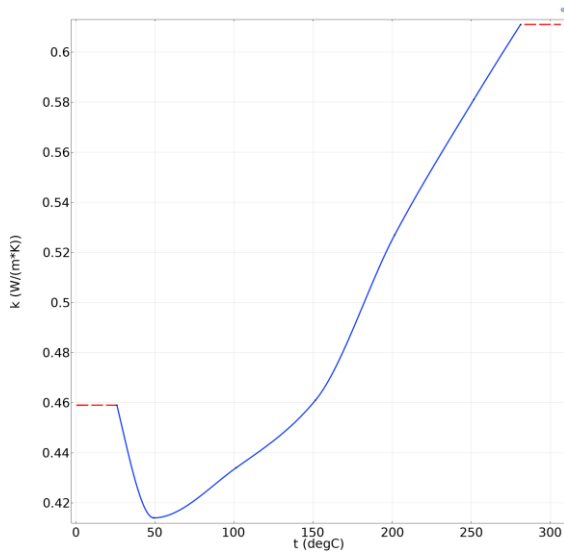


Figure 12. Temperature dependence for thermal conductivity k for PBGO sample.

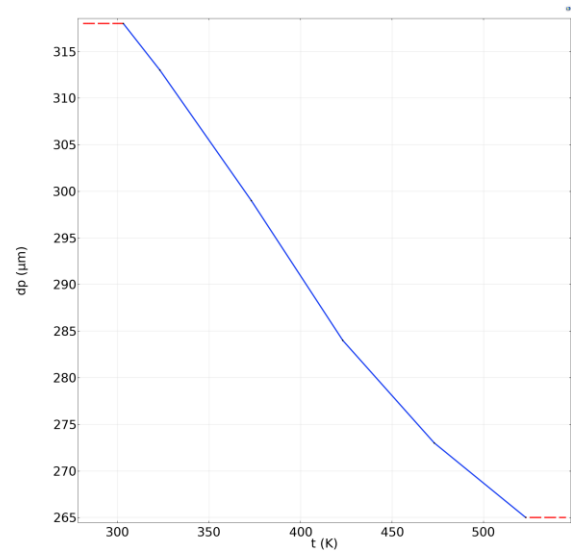


Figure 13. Temperature dependence for penetration depth d_p for PBGO sample.

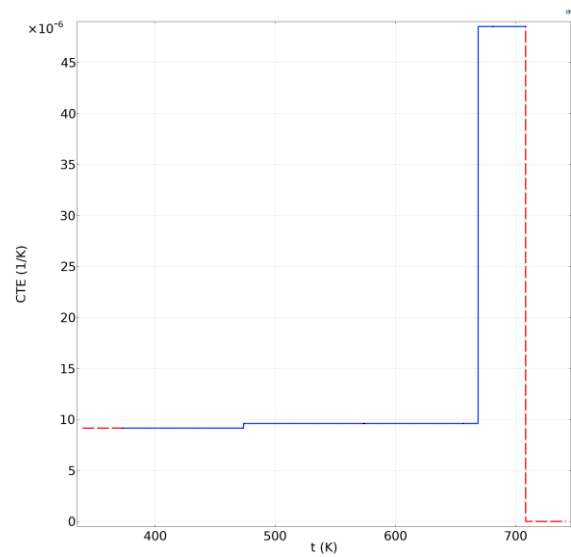


Figure 14. Temperature dependence for coefficient of thermal expansion CTE for PBGO sample.